Interdecadal Change of Tropical Cyclone Translation Speed during Peak Season in South China Sea: Observed Evidence, Model Results, and Possible Mechanism

KAIYUE SHAN,[a] PAO-SHIN CHU,[b] AND XIPING YU[c]

[a] *State Key Laboratory of Hydroscience and Engineering, Department of Hydraulic Engineering, Tsinghua University, Beijing, China*
[b] *Department of Atmospheric Sciences, School of Ocean and Earth Science and Technology, University of Hawai'i at Mānoa, Honolulu, Hawaii*
[c] *Department of Ocean Science and Engineering, Southern University of Science and Technology, Shenzhen, Guangdong Province, China*

(Manuscript received 17 September 2022, in final form 20 January 2023, accepted 23 February 2023)

ABSTRACT: Long-term variations in the translation speed of tropical cyclones (TCs) in the South China Sea (SCS) are examined based on five TC datasets from different institutions. TC translation speed during the TC peak season in the SCS shows an evident rhythm of interdecadal change throughout 1977–2020. This interdecadal change in TC translation speed in the SCS can be well reproduced by a newly developed trajectory model. The model results indicate that the interdecadal change in TC translation speed is primarily due to an interdecadal change in the steering flow in the SCS. Such an interdecadal change in the steering flow is closely related to an east–west shift of the subtropical high in the western North Pacific (WNP) ocean basin, which may be driven by the zonal sea surface temperature (SST) gradient between the north Indian (NI) and WNP ocean basins. A new index of the zonal SST gradient is proposed, which is shown to be effective for indicating the interdecadal change in east–west shift of subtropical high, and thus, the TC translation speed in the SCS.

SIGNIFICANCE STATEMENT: Identification of the prevailing trend of tropical cyclone activities due to climate change has been a challenging subject of scientific studies in recent years. This research focuses on the long-term variability of the tropical cyclone translation speed in the South China Sea. It is demonstrated that there is evidently an interdecadal rhythm for variation of the tropical cyclone translation speed in the South China Sea, and this variation can be well reproduced using a newly developed trajectory model. Based on the simulation results, the possible mechanism for this variation is also elucidated.

KEYWORDS: Tropical cyclones; Extreme events; Climate change; Decadal variability; Sea surface temperature

1. Introduction

The South China Sea (SCS) is a good example of marginal seas, which is surrounded by continents with dense populations and vulnerable to natural disasters (Liu and Gan 2017; Gan et al. 2022). Tropical cyclones (TCs) are the most destructive natural disasters in the SCS and have caused huge damage to surrounding regions (Zhang et al. 2009; Peduzzi et al. 2012; Shan and Yu 2021). A better understanding of the variability of TC activity in the SCS is important in order to reduce TC-related losses.

The TCs in the SCS generally show different characteristics (e.g., genesis, tracks, and intensity) than those in other regions (Wang et al. 2013; Li et al. 2017; Chang et al. 2020; Wang and Wang 2021). Previous studies showed that TC genesis frequency in the SCS shows an interdecadal change, with suppressed TC genesis in 1982–93 and 2003–15, but enhanced TC genesis in 1994–2002 (Wang et al. 2013; Li and Zhou 2014; Ha and Zhong 2015; Li et al. 2019). A similar interdecadal change in TC intensity in the SCS was also identified in a recent study (Zheng and Wang 2022). Along with TC frequency and intensity, TC translation speed is a major concern of the scientific community (Kim et al. 2020; Wang et al. 2020). TCs with low translation speed often cause more serious damage because the slower TCs move, the longer the lingering time, and the greater the impact of TC-related torrential rainfall as well as destructive winds (Emanuel 2017; Yamaguchi et al. 2020). For example, the slow movement of Typhoon Morakot in August 2009 produced 4-day accumulated rainfall of 2965 mm and killed more than 600 people in southern Taiwan Island (Lee et al. 2011). Moreover, the slowdown of TC movement increases the total momentum transferred from the TC to the underlying ocean waters. This leads to deeper vertical mixing in the upper ocean and enhances sea surface cooling, which eventually reduces the intensity of heat flux from the ocean to the TC, thereby inhibiting TC intensification (Lin et al. 2003; Chang et al. 2020). Long-term variations in TC translation speed have been investigated on the global and basinwide scales (Kossin 2018; Chan 2019; Moon et al. 2019; Lanzante 2019; Kim et al. 2020). However, little is known about how the translation speed of TCs in the SCS has changed.

In this study, long-term variations in TC translation speed in the SCS are investigated. TC translation speed in the SCS from 1977 to 2020 exhibits an evident interdecadal change based on five different TC datasets. A TC trajectory model (Shan and Yu 2020) will be used to compare the simulated

Denotes content that is immediately available upon publication as open access.

Corresponding author: Xiping Yu, yuxp@sustech.edu.cn

DOI: 10.1175/JCLI-D-22-0704.1

translation speed with the observed one in the SCS on the interdecadal time scale. The simulation indicates that the interdecadal change in TC translation speed is closely related to changes in steering flows in the SCS, which are associated with an east–west shift of subtropical high in the western North Pacific ocean basin. The regulation effect of the zonal sea surface temperature (SST) gradient between the north Indian (NI) and the western North Pacific (WNP) ocean basins is emphasized. A new index of the zonal SST gradient is constructed, which has a good performance in indicating the interdecadal change in TC translation speed in the SCS. This paper is organized as follows: there is a description of the data in section 2, the methodology used is described in section 3, results are presented in section 4, and the conclusions and discussion are in section 5.

2. Data

TC data (including 6-hourly TC position and intensity) are obtained from the Joint Typhoon Warning Center (JTWC), Japan Meteorological Agency (JMA), China Meteorological Administration–Shanghai Typhoon Institute (CMA), Hong Kong Observatory (HKO), and Advanced Dvorak Technique–Hurricane Satellite dataset (ADT-HURSAT; Kossin et al. 2013, 2020). The first four datasets are extracted from the International Best Track Archive for Climate Stewardship, version 4 (IBTrACSv4.0; Knapp et al. 2010), during 1977–2020 and the last is a new experimental dataset based on satellite infrared imagery analysis during 1981–2017. While using similar data sources, different institutions derive the TC datasets independently. The maximum sustained wind speed of TCs has been estimated with different definitions of the time interval in different datasets (Song et al. 2010; Wu and Zhao 2012; Zheng and Wang 2022). For example, JTWC uses 1-min average wind speed, CMA uses 2-min average wind speed, while both JMA and HKO prefer 10-min average wind speed. However, the differences in TC tracks among these datasets are negligibly small. Since our objective in this study is to examine whether any interdecadal change exists in the TC translation speed based on different datasets, but not in the TC intensity, no adjustment to these datasets is necessary. In fact, the dataset from JTWC is primarily used for investigation the long-term variability of TC translation speed in the SCS in this study, and the other datasets are used to further confirm the robustness of the phenomenon.

We only studied TCs reaching tropical storm intensity (maximum sustained wind speed > 34 kt; 1 kt ≈ 0.51 m s^{-1}) in the SCS (0°–25°N, 105°–120°E). TC translation speed is calculated at each 6-hourly observed position. The translation speed values along all TC tracks over the SCS are then averaged in the peak TC season (July–September) every year to produce the time series of TC translation speed. About half of the TCs occur in the peak TC season, and about 30% of TCs occur in the late TC season (October–December), which exhibit distinct characteristics from TCs in the peak TC season in previous studies (Li et al. 2019; Shi et al. 2020). In contrast to the interdecadal change in translation speed for TCs in the peak TC season, no significant change for TCs in the late TC season is observed.

Horizontal winds and geopotential heights are derived from the National Centers for Environmental Prediction–National Center for Atmosphere Research (NCEP–NCAR; Kalnay et al. 1996) reanalysis data, with a horizontal resolution of 2.5° × 2.5° and various pressure levels from 1000 to 10 hPa. Monthly mean data of SST with a horizontal resolution of 2° × 2° are derived from the Extended Reconstructed Sea Surface Temperature (ERSST), version 5 (Huang et al. 2017). The PDO index is obtained from the Joint Institute for the Study of the Atmosphere and Ocean of the University of Washington (https://www.ncei.noaa.gov/pub/data/cmb/ersst/v5/index/ersst.v5.pdo.dat).

3. Methods

A statistical changepoint analysis was applied in the time series of TC records to objectively identify whether there are pronounced shifts in the TC series (Elsner et al. 2000; Chu 2002). Specifically, a step function is used as an independent variable and a logarithmic transformation of TC rates is applied as a dependent variable for detecting abrupt shifts in the TC time series. As an example, two changepoints are found to be significant at $\alpha = 0.05$ level in annual TC frequency over the central North Pacific for the period of 1966–2000. Details of the method can be found in Chu (2002). The moving t test (Karl and Riebsame 1984), which is also a common method for detecting regime shifts, is used to examine the changepoint in the time series of SST index (Zhou et al. 2009; Zhao et al. 2018; Zheng and Wang 2022).

In the trajectory model, a TC is treated as a point vortex that moves from its genesis position at a translation speed, which is the sum of the large-scale steering flow and the beta drift. The estimation of the beta drift varies in different studies (Wu and Wang 2004; Emanuel et al. 2006; Zhao et al. 2009; Colbert and Soden 2012). Shan and Yu (2020) developed a semiempirical formula for the beta drift that reasonably represents the physical mechanism behind the beta drift and proposed a new trajectory model. To examine the performance of the TC trajectory model in the simulation of TC translation speed in the SCS, the translation speed of each historical TC over the WNP ocean basin is simulated during the peak TC season (July–September) during 1977–2020 and only TCs generated within or passing through the SCS are selected. Historical TC genesis locations from the JTWC dataset and the horizontal wind field from the NCEP–NCAR reanalysis dataset are used to drive the trajectory model. The annual mean translation speed of TCs in the SCS obtained from the simulated results is then compared with that derived from observed data.

To assess the relative contributions of the steering flow and beta drift to the variations in TC translation speed, an experiment based on the trajectory model is conducted by using the climatological mean of the beta drift during the period of 1977–2020. The climatological mean of the beta drift is calculated as the difference between the magnitudes of TC translation speed and steering flow derived from the observed data.

Steering flow is defined as the pressure-weighted tropospheric layer mean flow from the 850 to 300 hPa (Holland 1984; Wu et al. 2005; Chu et al. 2012) over each grid element

in the WNP ocean basin (0°–30°N, 100°E–180°). The subtropical high in the WNP is commonly represented by the geopotential height of 500-hPa (Chu et al. 2012; He et al. 2015, 2018; Wu and Wang 2015; Li et al. 2019).

4. Results

a. Interdecadal variation in TC translation speed

Figure 1 shows the time series of TC translation speed in the SCS in the peak TC season (July–September) during 1977–2020 obtained from the JTWC dataset. A striking interdecadal change in TC translation speed is observed, with three epochs being identified. The first and third epochs are characterized by high translation speed, while a considerable decrease (approximately 20% below average) is noted in the second epoch, which runs from the early 1990s to the early 2000s. To further ascertain this interdecadal change, the time series of TC translation speed is examined based on other four TC datasets, including the JMA, CMA, and HKO datasets and ADT-HURSAT (see methods section). The four datasets consistently show the same interdecadal change (Fig. 2). While using similar data sources, different operational institutions derive the TC datasets independently. The agreement among all five TC datasets lends credence to results based on the JTWC dataset.

We use a statistical analysis method by Elsner et al. (2000) and Chu (2002) to examine the statistical significance of the interdecadal change in TC translation speed in the SCS. Supported by all five TC datasets from different institutions, the first abrupt change year of TC translation speed occurs universally in 2003, with a significant level at 10% (Fig. 3a). The second abrupt change year of the TC translation speed occurs in the early 1990s, with a slight difference in different TC datasets (Fig. 3b). For example, it occurs in 1991 in JTWC dataset, in 1990 in JMA dataset and ADT-HURSAT, and in 1993 in HKO dataset. The second abrupt change year is not significant in CMA dataset. The difference between different TC datasets may be largely due to discrepancies in the TC estimation methodology (Knapp et al. 2010) and changes in the CMA methodology (Ying et al. 2014). To obtain a consensus regarding the interdecadal change in TC translation speed, three epochs are identified, including two high translation speed epochs (epoch 1: 1977–90; and epoch 3: 2003–20) and a low translation speed epoch (epoch 2: 1994–2002). The mean values of TC translation speed are 4.6 m s^{-1} in epoch 1, 3.8 m s^{-1} in epoch 2, and 4.9 m s^{-1} in epoch 3, respectively (dashed lines shown in Fig. 1), highlighting the interdecadal change.

Recently, a TC trajectory model was put forward by Shan and Yu (2020) that did a better job of simulating the spatial pattern of TC occurrence frequency as well as the prevailing tracks over the WNP ocean basin when compared with other models. To verify the performance of this TC trajectory model in simulating TC translation speed in the SCS, the translation speed of each historical TC over the WNP ocean basin is simulated in the prescribed period and only the TCs generated within or passing through the SCS are selected. For those TCs originating in WNP and then moving to the SCS, only the periods when TCs live in the SCS are considered. As

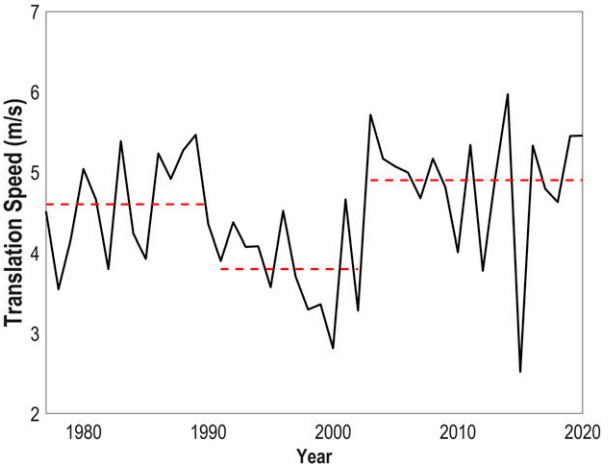

FIG. 1. Time series (black solid line) of TC translation speed in the SCS in July–September during 1977–2020 obtained from the JTWC dataset. The red dashed lines denote the means in the respective epochs.

shown in Fig. 4a, the interdecadal change in TC translation speed in the SCS is well reproduced based on this trajectory model. The mean values of TC translation speed obtained from the simulated results are 4.7 m s^{-1} in epoch 1, 3.8 m s^{-1} in epoch 2, and 4.9 m s^{-1} in epoch 3, which is in agreement with the relevant ones derived from observed data. Thus, the application of the TC trajectory model is a suitable tool for understanding the interdecadal change in TC translation speed in the SCS.

TC translation speed is mainly governed by the large-scale steering flow and beta drift (Holland 1984; Chan 2005). The steering flow is generally calculated as the pressure-weighted tropospheric layer-mean flows (Holland 1984; Chu et al. 2012), while the beta drift refers to a minor deviation from the steering flow that arises from nonlinear interactions among the TC system, planetary vorticity gradient, and large-scale environmental flow (Fiorino and Elsberry 1989; Chan 2005). The next step is to evaluate the relative contributions of the steering flow and the beta drift to translation speed. To do this, a sensitivity experiment based on the TC trajectory model is performed in which the climatological mean value of the beta drift during the period of 1977–2020 is used (Fig. 4b). The difference between the TC translation speeds obtained from the simulation and the sensitivity experiment can be readily obtained. Only slight changes in the difference of TC translation speed can be observed, with a mean value of 0.2 m s^{-1} in epoch 1, 0.3 m s^{-1} in epoch 2, and 0.1 m s^{-1} in epoch 3, respectively. It is thus suggested that the interdecadal change in TC translation speed is mainly related to the changes in steering flows, while changes in the beta drift play an insignificant role.

b. Physical mechanism

Figure 5 shows the steering flow velocity and its anomaly relative to the climatological mean during the three epochs. For epoch 1 (Fig. 5a), southwesterly steering flows are noted over the southern part (5°–15°N) of the SCS in the peak TC

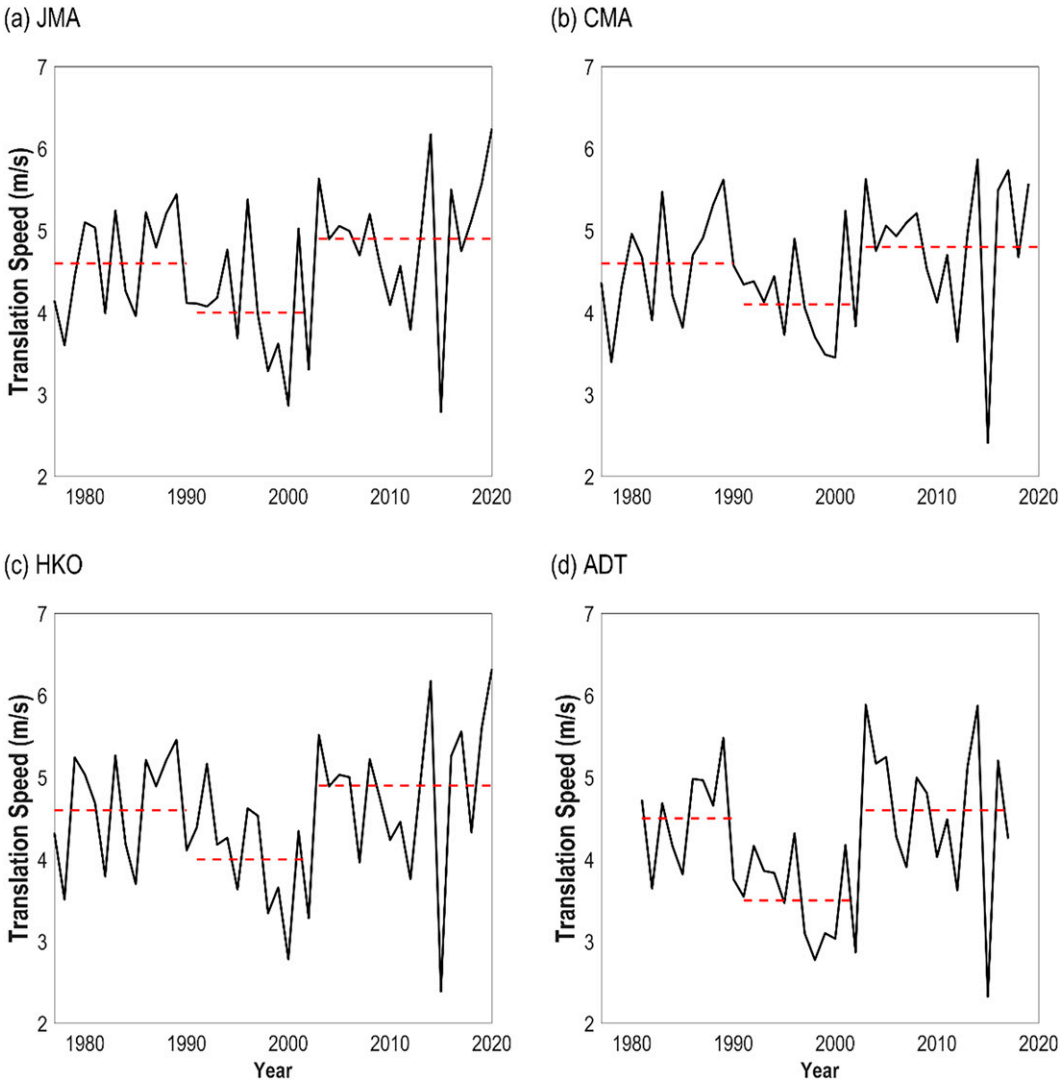

FIG. 2. As in Fig. 1, but for the time series of TC translation speed obtained from the (a) JMA, (b) CMA, (c) HKO, and (d) ADT datasets.

season (July–September), while strong southeasterly steering flows are found over the northern part (15°–25°N) of the SCS and the western part of the WNP ocean basin. For the low translation speed epoch of 1994–2002 (epoch 2; Fig. 5b), the pattern of the steering flow is similar to that in epochs 1 and 3 (Figs. 5a,c); however, there is a marked decrease in the steering flows (relative to its climatological mean; blue shading) in epoch 2. The southeasterly steering flows over the northern part of the SCS are reduced in strength and turn more southerly in epoch 2, because the reduction is mainly concentrated in its zonal component. Also noticeable in Fig. 5b is the decreased southwesterly steering flows over the southern part of the SCS. In contrast, both the southeasterly steering flows over the northern part of the SCS and the southwesterly steering flows over the southern part show are enhanced (red shading) in epochs 1 and 3. These results suggest that the interdecadal change in TC translation speed is closely associated with changes in the large-scale steering flows during the three epochs. The dominant role of the large-scale steering flow in moderating TC translation speed is also consistent with previous studies (Wu et al. 2005; Sun et al. 2015; Wu and Chen 2016; Shan and Yu 2021).

The steering flow in the SCS is largely controlled by the subtropical high in the WNP. Stronger steering flows would be induced by larger pressure gradient to the southwest of the subtropical high, which is closely related to the westward extension of the subtropical high, and vice versa (Chan and Gray 1982; Ho et al. 2004; Wu et al. 2005; Chu et al. 2012). To investigate the effect of the subtropical high, the distributions of the 500-hPa subtropical high pressure in the three epochs are shown in Fig. 6. Relative to epochs 1 and 3, there is an eastward retreat of the subtropical high pressure region over the WNP in epoch 2. The western edge of the subtropical high, as represented by the 5865-gpm contour (Li et al. 2019),

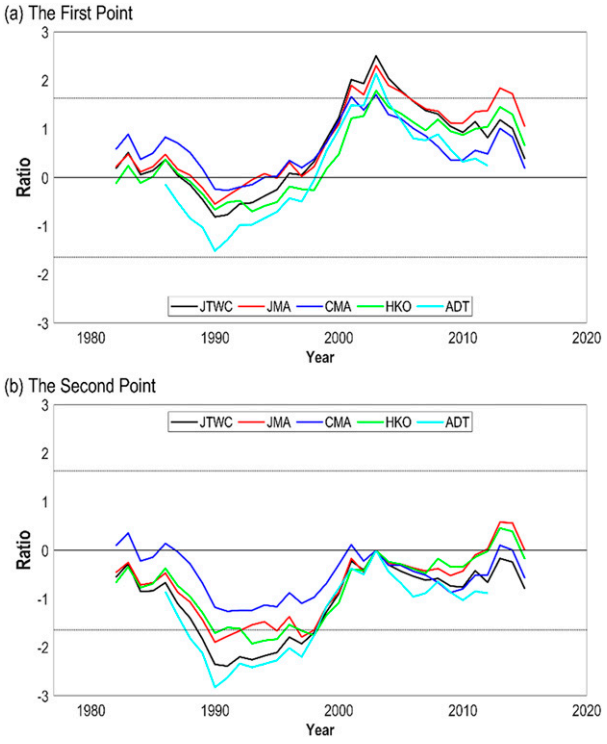

FIG. 3. Significance index (ratio) of TC translation speed for (a) the first changepoint and (b) the second changepoint. The five solid lines represent the five TC datasets. The horizontal dashed lines indicate the 10% significant level of changepoint analysis.

shifts from approximately 105°E in epoch 1 to 115°E in epoch 2. As the subtropical high in the WNP becomes weak and withdraws eastward away from the SCS in epoch 2, the pressure gradient to the southwestern side of the subtropical high becomes small, thereby inducing weaker steering flows. In epoch 3, the subtropical high pressure region extends westward again (the western edge is near 95°E) and leads to stronger steering flows. Noticeably, the westward extension of the subtropical high in the WNP corresponds to the strong subtropical high, and vice visa (Tu et al. 2009; Chu et al. 2012; Li and Zhou 2014).

The above analysis suggests that the interdecadal variation in TC translation speed is accompanied by remarkable changes in the steering flow in the SCS, which are associated with the subtropical high in the WNP during the three epochs. The next question we need to address is what is responsible for the interdecadal variation of the subtropical high pressure. Many recent studies emphasize the dominance of the zonal SST gradient between the NI and the WNP ocean basins on TC activity in the SCS by regulating the subtropical high (Li and Zhou 2014; Li et al. 2019; Zheng and Wang 2022). The zonal SST gradient between the NI and the WNP largely controls the east–west shift of the subtropical high in the WNP on the interdecadal scale, with the positive (negative) zonal SST gradient corresponding to the westward (eastward) shift of the subtropical high pressure system. In contrast, the relationship between TC activity and the local SST over the SCS or the SST

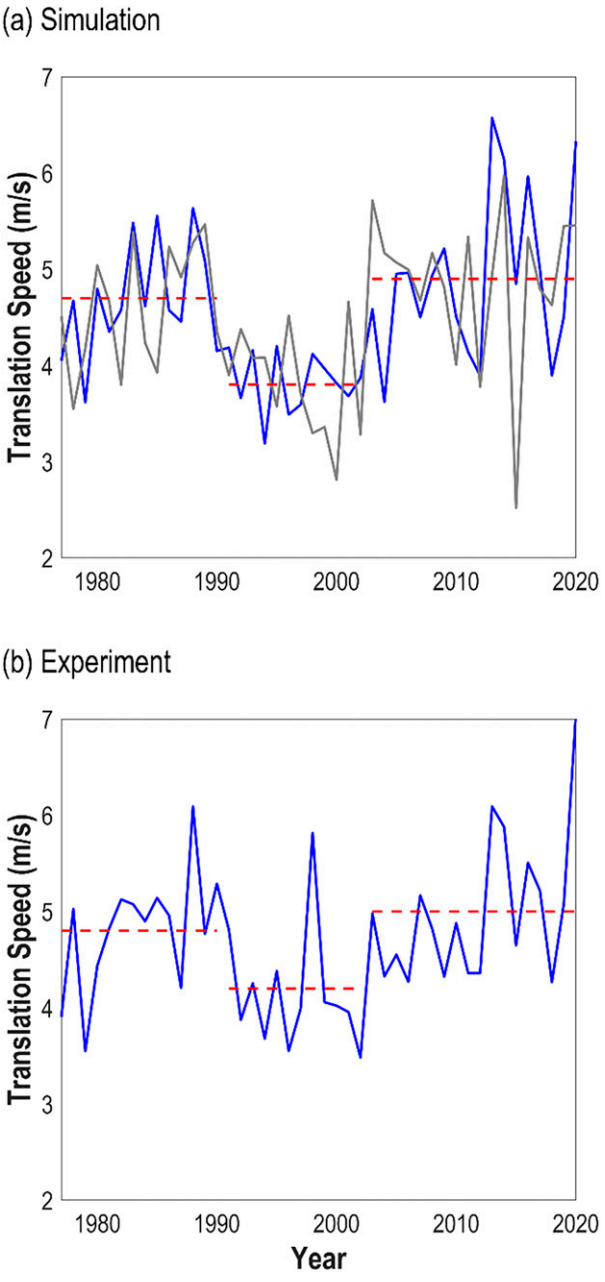

FIG. 4. (a) Time series of TC translation speed in the SCS obtained from the trajectory model simulation (blue solid line); red dashed lines denote the means in the respective epochs; gray solid line denotes the time series of TC translation speed obtained from the JTWC dataset (Fig. 1). (b) Time series of TC translation speed in the SCS obtained from the sensitivity experiment (blue solid line); red dashed lines denote the means in the respective epochs.

over each individual ocean is weak (Chan and Liu 2004; Li and Zhou 2014).

The SST anomaly over the NI and WNP during the peak TC season in epoch 1 is shown in Fig. 7a, with cooler SST relative to its climatological mean over both the NI and the WNP ocean basins. Noticeably, the NI ocean basin is

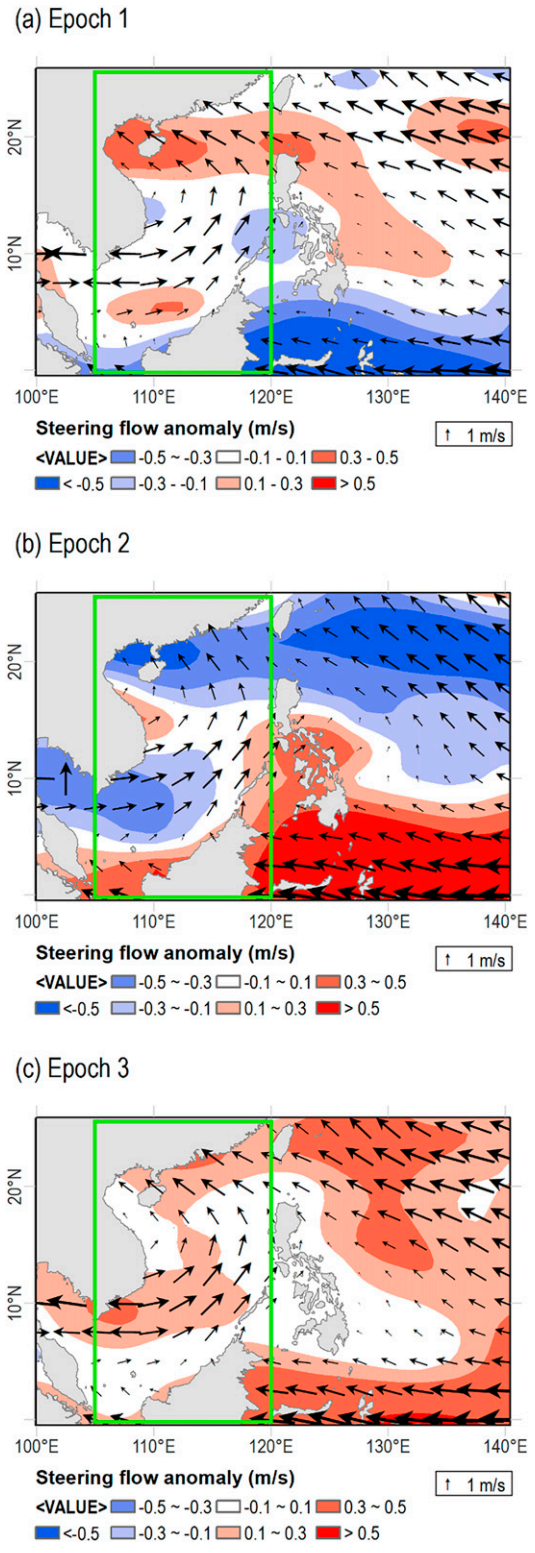

FIG. 5. Steering flow velocity (vectors; m s^{-1}) and its anomaly relative to the climatological mean (shading; m s^{-1}) in July–September during the (a) epoch 1 (1977–90), (b) epoch 2 (1994–2002), and (c) epoch 3 (2003–20). The green box is the region of SCS (0°–25°N, 105°–120°E).

generally warmer than the WNP in July–September. As a consequence, the zonal SST gradient between the NI and the WNP ocean basins in epoch 1 is positive. The SST over the WNP became warmer in epoch 2 (Fig. 7b) and a negative zonal SST gradient between the NI and the WNP ocean basins was observed. The zonal SST gradient turns to be positive in epoch 3 (Fig. 7c), as the SST anomaly becomes positive over the NI ocean basin. The pattern of a warmer NI ocean and cooler WNP ocean may lead to the eastward retreat of subtropical high (Fig. 6b) by suppressing the wind–evaporation/entrainment–SST (WES) feedback and inducing relatively low-pressure anomalies at the western edge region of the subtropical high (Wu et al. 2009; Xie et al. 2009; Li et al. 2019). Furthermore, a recent study has indicated that the warming NI ocean could induce anomalous anticyclone and strengthens the subtropical high over WNP by forcing the atmospheric Kelvin wave to propagate into the equatorial western Pacific (Kim and Kug 2021).

To quantify the effect of the zonal SST gradient between the NI and WNP ocean basins, a zonal SST gradient index is constructed. This index is calculated based on the SST difference between the NI (0°–20°N, 50°–100°E) and the WNP (0°–40°N, 120°–150°E) ocean basins. As shown in Fig. 7d, the zonal SST gradient index serves as a good indicator for the interdecadal change in TC translation speed in the SCS. The moving t test (Zhou et al. 2009; Zhao et al. 2018) is employed to detect whether the new zonal SST gradient index undergoes an interdecadal change (Fig. 8). It is clear that the new zonal SST gradient index has a significant interdecadal change, with the abrupt change years in 1994 and 2002. Such an interdecadal change in the new zonal SST gradient index is consistent with the interdecadal variation of east–west shift of subtropical high. In epoch 2, the negative zonal SST gradient between the NI and the WNP is associated with the low TC translation speed in the SCS due to an eastward retreat of subtropical high and weakened steering flows. In contrast, the positive zonal SST gradient during epochs 1 and 3 is generally favorable for high TC translation speed in the SCS. These results are consistent with previous studies, which focused on the interdecadal variations in TC number (Wang et al. 2013; Li and Zhou 2014; Ha and Zhong 2015; Li et al. 2019) and TC intensity (Zheng and Wang 2022) in the SCS. The abrupt change years in our study are the same as in those previous studies.

5. Conclusions and discussion

This study focused on the interdecadal variation in TC translation speed in the SCS and its relation with the relevant environmental factors. It is clearly shown that TC translation speed in the SCS from 1977 to 2020 exhibits an evident interdecadal change, with three different epochs being identified. The first and third epochs are marked by high translation speeds, while an abrupt decrease in translation speed is noted in the second epoch from the early 1990s to the early 2000s (approximately 20% below average). The robustness of the interdecadal change in TC translation speed is confirmed by the other four TC datasets. Based on a newly developed trajectory model, the interdecadal change in TC translation speed in the SCS can be well reproduced. Furthermore, the

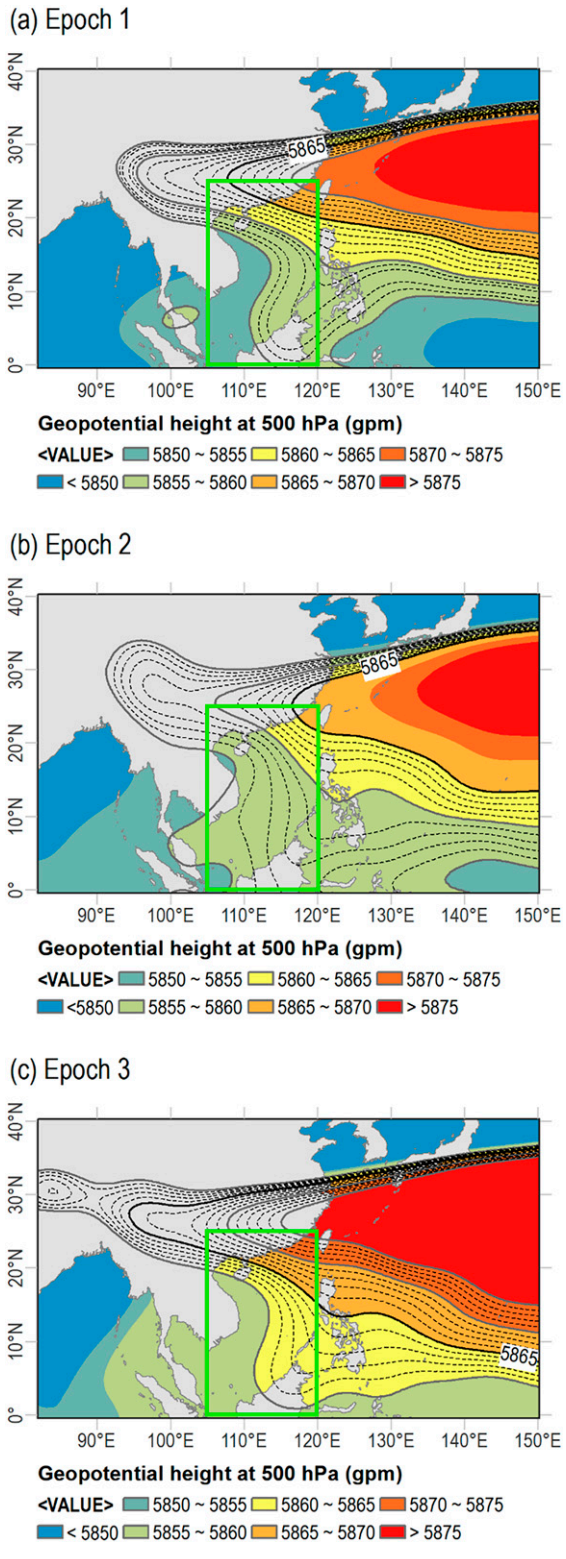

FIG. 6. Geopotential height of 500-hPa (shading; gpm) during July–September in the (a) epoch 1 (1977–90), (b) epoch 2 (1994–2002), and (c) epoch 3 (2003–20). The black solid line represents the 5865-gpm contour. The dashed lines represent the contours with the interval of 1-gpm. The green box is the region of SCS.

sensitivity experiment indicates that the interdecadal change in TC translation speed results primarily from changes in the steering flow in the SCS. Both the southeasterly steering flow over the northern part of the SCS and southwesterly steering flow over the southern part are reduced in strength in epoch 2, while the steering flow is relatively stronger in epoch 1 and 3. The interdecadal change in the steering flow in the SCS can be largely attributed to the east–west shift of the subtropical high in the WNP. When the subtropical high in the WNP becomes weak and withdraws eastward away from the SCS, the pressure gradient around the southwestern side of the subtropical high is small, thereby inducing weak steering flows, and vice versa. These variations are found to be driven by the zonal SST gradient between the NI and WNP ocean basins. A new index of the zonal SST gradient is proposed that does a good job of indicating the interdecadal variation of east–west shift of subtropical high, and thus, the TC translation speed in the SCS.

Figure 6c shows an extraordinarily strong subtropical high in the WNP during epoch 3. Relative to the subtropical high in epoch 1 (Fig. 6a), the westward extension of the subtropical high is obvious, with the western edge shifting from 105°E in epoch 1 to 95°E in epoch 3. Such a westward extension of the subtropical high may be related to global warming (He et al. 2015, 2018; Wu and Wang 2015; Li et al. 2019), which induces a global-scale rise in the geopotential height. To remove this effect, the 500-hPa geopotential height after subtracting the zonal mean averaged over 0°–40°N is calculated (Fig. 9), using the approach proposed by Wu and Wang (2015). For clarity, the 0-gpm contour is highlighted, indicating the position of the subtropical high pressure region after subtracting the zonal mean. The 0-gpm contour in epoch 1 (Fig. 8a) is close to the position of the 5865-gpm contour of the subtropical high in the same epoch (Fig. 6a), while the 0-gpm contour in epochs 2 and 3 (Figs. 8b,c) is located to the east of the 5865-gpm contour. The westward extension of the subtropical high shown in Fig. 6 disappears. It is worth noting that the east–west shift of subtropical high in the WNP is still evident when subtracting the zonal mean of geopotential height, with the eastward retreat of subtropical high in epoch 2 and the westward extension in epochs 1 and 3. Our results suggest that an index that removes the global-scale rise of the geopotential height in response to global warming may be more appropriate to characterize the east–west shift of the subtropical high in the WNP.

While focusing on the interdecadal change in SCS TC frequency, Li and Zhou (2014) found that the positive zonal SST gradient between the NI and WNP ocean basins in summer (June–August) tends to suppress TC genesis in the SCS in 1979–93 and 2003–10, whereas the negative zonal SST gradient is favorable for SCS TC formation in 1994–2002. Li and Zhou (2014) also suggested a zonal SST gradient index, which is defined as the summer SST difference between the NI and WNP at low latitudes (5°–20°N); however, this index is not in good agreement with the interdecadal change in the TC translation speed in our study. Consequently, we propose a new zonal SST gradient index, which does a better job of indicating the interdecadal change of TC translation speed in the SCS. Note that the SST gradient is examined during the peak TC season (July–September) rather than the conventional

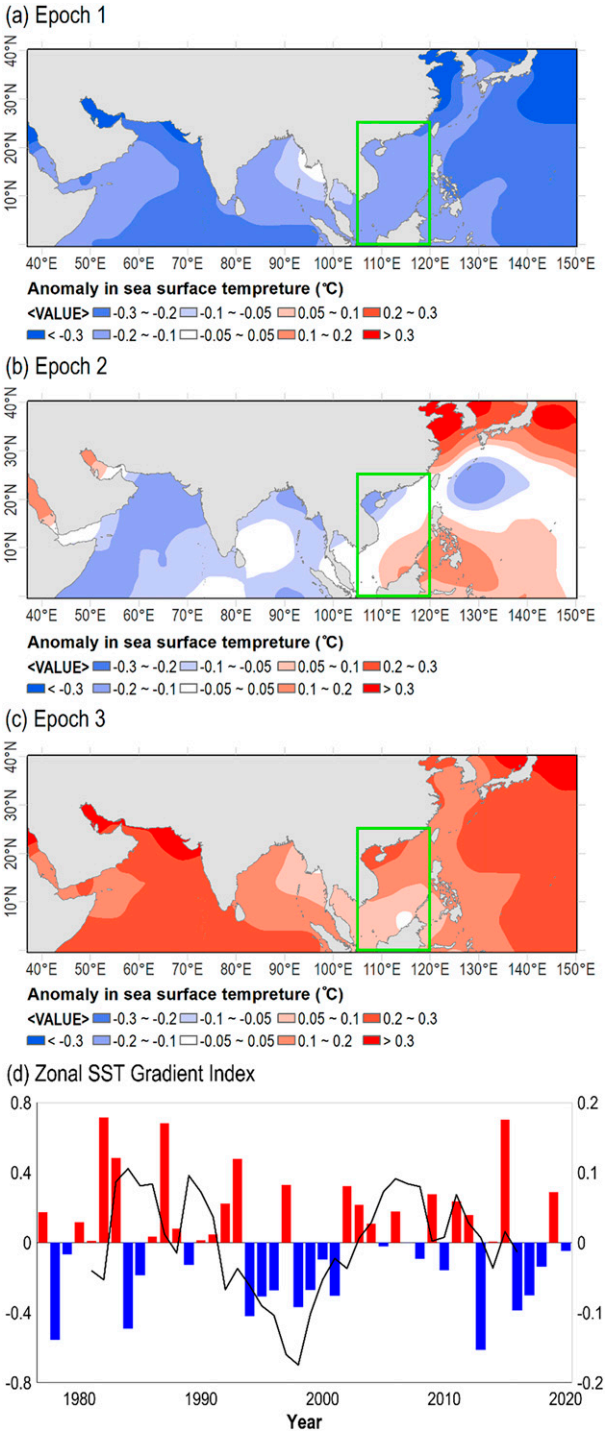

FIG. 7. Sea surface temperature anomaly relative to its climatological mean (shading; °C) in July–September during the (a) epoch 1 (1977–90), (b) epoch 2 (1994–2002), and (c) epoch 3 (2003–20). The green box is the region of SCS (0°–25°N, 105°–120°E). (d) Time series of the zonal SST gradient index (bars) between the north Indian Ocean (0°–20°N, 50°–100°E) and the western North Pacific (0°–40°N, 120°–150°E) in July–September during 1977–2020. The black solid line represents the 9-yr running mean.

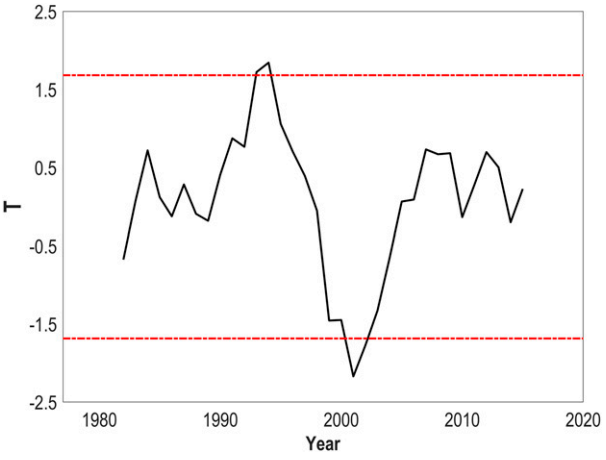

FIG. 8. The T values for time series of the new zonal SST gradient index. The horizontal dashed lines indicate the significant level of 10% in moving t test.

summertime. The definition of the WNP in the new index is extended to higher latitudes (0°–40°N), given the key role of ocean temperature in heating the atmospheric column, elevating the pressure level, and ultimately strengthening the subtropical high in the WNP (Emanuel et al. 1994).

There exist possible contributions from global warming and natural variability to the new zonal SST gradient index. To verify such a possibility, variations of SST in the two ocean basins and of the Pacific decadal oscillation (PDO) index are studied. The linear trends of SST in the two ocean basins during 1977–2020 are found to be almost the same, with the rate of 0.17°C decade^{-1} in NI and 0.18°C decade^{-1} in WNP. Combined with the fact that the global-scale rise of the geopotential height in response to global warming contributes little to the east–west shift of the subtropical high as shown in Fig. 9, the similar trends of SST over NI and WNP suggest that global warming may have little effect on the interdecadal change in TC translation speed in the SCS during the period of study.

The relationship between the new zonal SST gradient index and the PDO index is examined by extending the period of study to 1950 (Fig. 10). The zonal SST gradient index shows an abrupt decrease in the early 1990s followed by an abrupt increase in the early 2000s, while the PDO index shifts to its negative phase near the 2000s. The correlation coefficients of the two times series reach the peak with a time lag of −10 years, suggesting that the zonal SST gradient index may lead the PDO index by approximately 10 years. This phase lead of the zonal SST gradient index to the PDO index may be associated with the air–sea interaction between NI and WNP ocean basins. Previous studies have claimed that the SST changes in NI could induce a subsequent phase shift of the SST mode in WNP through moderating the Walker circulation (Zhou et al. 2009; Wang 2019).

Variablity of TC translation speed in the SCS in the late TC season (October–December) is also investigated. No significant change in translation speed for TCs in the late TC season is observed as its mean value is 4.2 m s^{-1} in epoch 1, 4.1 m s^{-1} in epoch 2, and 4.2 m s^{-1} in epoch 3. In the late TC season, unlike in the peak TC season discussed before, the subtropical high

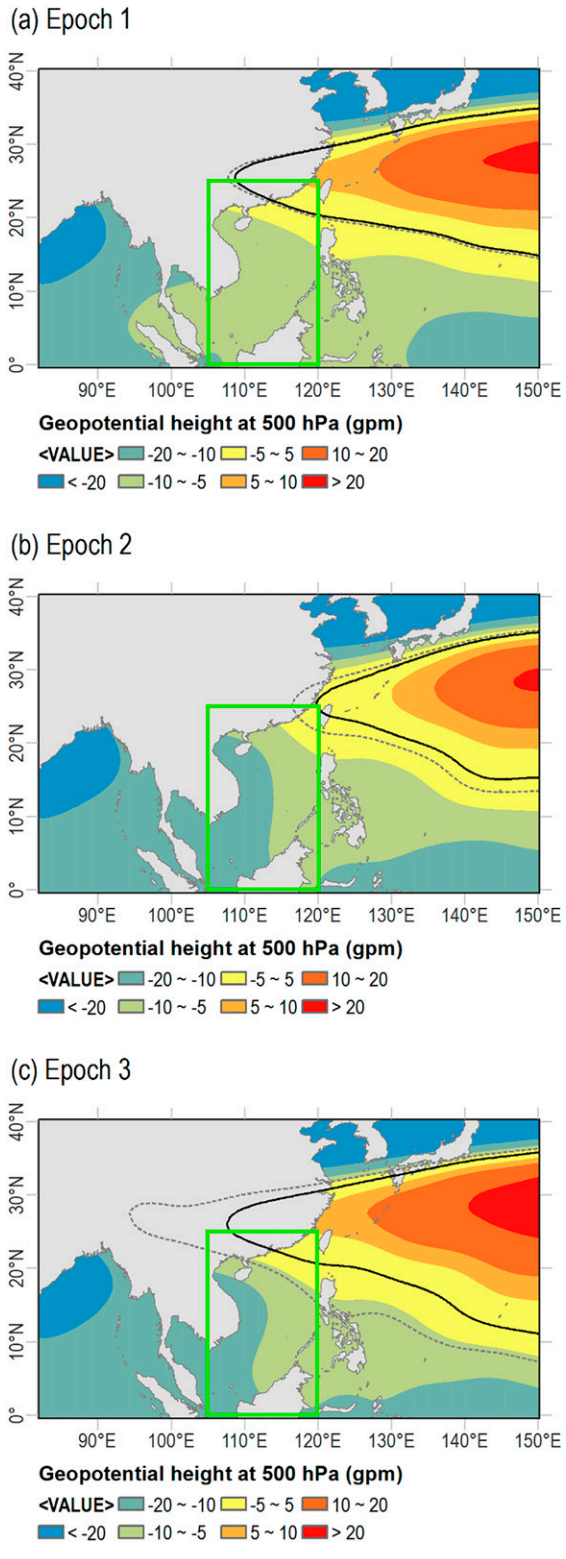

FIG. 9. As in Fig. 6, but for the 500-hPa geopotential height after the zonal mean averaged over 0°–40°N is subtracted. The black solid line represents the 0-gpm contour. The gray dashed line is the same as the 5865-gpm contour in Fig. 6.

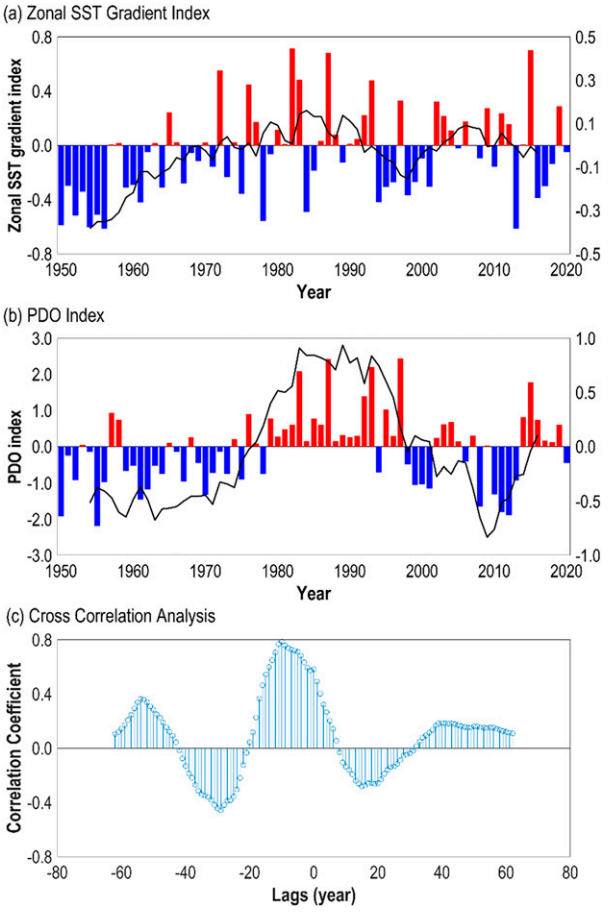

FIG. 10. (a) Time series of the zonal SST gradient index (bars) in July–September during 1950–2020. The black solid line represents the 9-yr running mean. (b) As in (a), but for the PDO index. (c) The correlation coefficients of the two times series based on cross-correlation analysis.

becomes stronger and extends more westward to the SCS during all three epochs (Tu et al. 2009; Li et al. 2019). A strong and steady subtropical high does not cause any significant change in the steering flow, which may be the possible reason for the lack of significant change in translation speed of TCs in the late TC season.

Acknowledgments. This research is supported by the National Natural Science Foundation of China (NSFC) under Grants 11732008 and 12102231.

Data availability statement. The data that support the findings of this study are all openly available. In particular, the tropical cyclone best-track data are available at https://www.ncdc.noaa.gov/ibtracs/index.php?name=ib-v4-access.

REFERENCES

Chan, J. C. L., 2005: The physics of tropical cyclone motion. *Annu. Rev. Fluid Mech.*, **37**, 99–128, https://doi.org/10.1146/annurev.fluid.37.061903.175702.

——, and W. M. Gray, 1982: Tropical cyclone movement and surrounding flow relationships. *Mon. Wea. Rev.*, **110**, 1354–1374, https://doi.org/10.1175/1520-0493(1982)110<1354:TCMASF>2.0.CO;2.

——, and K. S. Liu, 2004: Global warming and western North Pacific typhoon activity from an observational perspective. *J. Climate*, **17**, 4590–4602, https://doi.org/10.1175/3240.1.

Chan, K. T. F., 2019: Are global tropical cyclones moving slower in a warming climate. *Environ. Res. Lett.*, **14**, 104015, https://doi.org/10.1088/1748-9326/ab4031.

Chang, Y.-T., I.-I. Lin, H. C. Huang, Y.-C. Laio, and C.-C. Lien, 2020: The association of typhoon intensity increase with translation speed increase in the South China Sea. *Sustainability*, **12**, 939, https://doi.org/10.3390/su12030939.

Chu, P.-S., 2002: Large-scale circulation features associated with decadal variations of tropical cyclone activity over the central North Pacific. *J. Climate*, **15**, 2678–2689, https://doi.org/10.1175/1520-0442(2002)015<2678:LSCFAW>2.0.CO;2.

——, J.-H. Kim, and Y. R. Chen, 2012: Have steering flows in the western North Pacific and the South China Sea changed over the last 50 years? *Geophys. Res. Lett.*, **39**, L10704, https://doi.org/10.1029/2012GL051709.

Colbert, A. J., and B. J. Soden, 2012: Climatological variations in North Atlantic tropical cyclone tracks. *J. Climate*, **25**, 657–673, https://doi.org/10.1175/JCLI-D-11-00034.1.

Elsner, J. B., T. Jagger, and X.-F. Niu, 2000: Changes in the rates of North Atlantic major hurricane activity during the 20th century. *Geophys. Res. Lett.*, **27**, 1743–1746, https://doi.org/10.1029/2000GL011453.

Emanuel, K., 2017: Assessing the present and future probability of Hurricane Harvey's rainfall. *Proc. Natl. Acad. Sci. USA*, **114**, 12 681–12 684, https://doi.org/10.1073/pnas.1716222114.

——, S. Ravela, E. Vivant, and C. Risi, 2006: A statistical deterministic approach to hurricane risk assessment. *Bull. Amer. Meteor. Soc.*, **87**, 299–314, https://doi.org/10.1175/BAMS-87-3-299.

Emanuel, K. A., J. D. Neelin, and C. S. Bretherton, 1994: On large-scale circulations in convecting atmospheres. *Quart. J. Roy. Meteor. Soc.*, **120**, 1111–1143, https://doi.org/10.1002/qj.49712051902.

Fiorino, M., and R. L. Elsberry, 1989: Some aspects of vortex structure related to tropical cyclone motion. *J. Atmos. Sci.*, **46**, 975–990, https://doi.org/10.1175/1520-0469(1989)046<0975:SAOVSR>2.0.CO;2.

Gan, J., H. Kung, Z. Cai, Z. Liu, C. Hui, and J. Li, 2022: Hotspots of the stokes rotating circulation in a large marginal sea. *Nat. Commun.*, **13**, 2223, https://doi.org/10.1038/s41467-022-29610-z.

Ha, Y., and Z. Zhong, 2015: Decadal change of tropical cyclone activity over South China Sea around 2002/2003. *J. Climate*, **28**, 5935–5951, https://doi.org/10.1175/JCLI-D-14-00769.1.

He, C., T. Zhou, A. Lin, B. Wu, D. Gu, C. Li, and B. Zheng, 2015: Enhanced or weakened western North Pacific subtropical high under global warming? *Sci. Rep.*, **5**, 16771, https://doi.org/10.1038/srep16771.

——, A. Lin, D. Gu, C. Li, B. Zheng, B. Wu, and T. Zhou, 2018: Using eddy geopotential height to measure the western North Pacific subtropical high in a warming climate. *Theor. Appl. Climatol.*, **131**, 681–691, https://doi.org/10.1007/s00704-016-2001-9.

Ho, C.-H., J.-J. Baik, J.-H. Kim, D.-Y. Gong, and C.-H. Sui, 2004: Interdecadal changes in summertime typhoon tracks. *J. Climate*, **17**, 1767–1776, https://doi.org/10.1175/1520-0442(2004)017<1767:ICISTT>2.0.CO;2.

Holland, G. J., 1984: Tropical cyclone motion: A comparison of theory and observation. *J. Atmos. Sci.*, **41**, 68–75, https://doi.org/10.1175/1520-0469(1984)041<0068:TCMACO>2.0.CO;2.

Huang, B., and Coauthors, 2017: Extended Reconstructed Sea Surface Temperature, version 5 (ERSSTv5): Upgrades, validations, and intercomparisons. *J. Climate*, **30**, 8179–8205, https://doi.org/10.1175/JCLI-D-16-0836.1.

Kalnay, E., and Coauthors, 1996: The NCEP/NCAR 40-Year Reanalysis Project. *Bull. Amer. Meteor. Soc.*, **77**, 437–472, https://doi.org/10.1175/1520-0477(1996)077<0437:TNYRP>2.0.CO;2.

Karl, T. R., and W. E. Riebsame, 1984: The identification of 10- to 20-year temperature and precipitation fluctuations in the contiguous United States. *J. Climate Appl. Meteor.*, **23**, 950–966, https://doi.org/10.1175/1520-0450(1984)023<0950:TIOTYT>2.0.CO;2.

Kim, S., and J.-S. Kug, 2021: Delayed impact of Indian Ocean warming on the East Asian surface temperature variation in boreal summer. *J. Climate*, **34**, 3255–3270, https://doi.org/10.1175/JCLI-D-20-0691.1.

Kim, S.-H., I.-J. Moon, and P.-S. Chu, 2020: An increase in global trends of tropical cyclone translation speed since 1982 and its physical causes. *Environ. Res. Lett.*, **15**, 094084, https://doi.org/10.1088/1748-9326/ab9e1f.

Knapp, K. R., M. C. Kruk, D. H. Levinson, H. J. Diamond, and C. J. Neumann, 2010: The International Best Track Archive for Climate Stewardship (IBTrACS): Unifying tropical cyclone data. *Bull. Amer. Meteor. Soc.*, **91**, 363–376, https://doi.org/10.1175/2009BAMS2755.1.

Kossin, J. P., 2018: A global slowdown of tropical-cyclone translation speed. *Nature*, **558**, 104–107, https://doi.org/10.1038/s41586-018-0158-3.

——, T. L. Olander, and K. R. Knapp, 2013: Trend analysis with a new global record of tropical cyclone intensity. *J. Climate*, **26**, 9960–9976, https://doi.org/10.1175/JCLI-D-13-00262.1.

——, K. R. Knapp, T. L. Olander, and C. S. Velden, 2020: Global increase in major tropical cyclone exceedance probability over the past four decades. *Proc. Natl. Acad. Sci. USA*, **117**, 11 975–11 980, https://doi.org/10.1073/pnas.1920849117.

Lanzante, J. R., 2019: Uncertainties in tropical-cyclone translation speed. *Nature*, **570**, E6–E15, https://doi.org/10.1038/s41586-019-1223-2.

Lee, C. S., C. C. Wu, T. C. C. Wang, and R. L. Elsberry, 2011: Advances in understanding the "perfect monsoon-influenced typhoon": Summary from international conference on Typhoon Morakot (2009). *Asia-Pac. J. Atmos. Sci.*, **47**, 213–222, https://doi.org/10.1007/s13143-011-0010-2.

Li, H., F. Xu, J. Sun, Y. Lin, and J. S. Wright, 2019: Subtropical high affects interdecadal variability of tropical cyclone genesis in the South China Sea. *J. Geophys. Res. Atmos.*, **124**, 6379–6392, https://doi.org/10.1029/2018JD029874.

Li, R. C. Y., and W. Zhou, 2014: Interdecadal change in South China Sea tropical cyclone frequency in association with zonal sea surface temperature gradient. *J. Climate*, **27**, 5468–5480, https://doi.org/10.1175/JCLI-D-13-00744.1.

——, ——, C. M. Shun, and T. C. Lee, 2017: Change in destructiveness of landfalling tropical cyclones over China in recent decades. *J. Climate*, **30**, 3367–3379, https://doi.org/10.1175/JCLI-D-16-0258.1.

Lin, I.-I., W. T. Liu, C.-C. Wu, J. C. H. Chiang, and C.-H. Sui, 2003: Satellite observations of modulation of surface winds by typhoon-induced upper ocean cooling. *Geophys. Res. Lett.*, **30**, 1131, https://doi.org/10.1029/2002GL015674.

Liu, Z., and J. Gan, 2017: Three-dimensional pathways of water masses in the South China Sea: A modeling study. *J. Geophys. Res. Oceans*, **122**, 6039–6054, https://doi.org/10.1002/2016JC012511.

Moon, I.-J., S.-H. Kim, and J. C. L. Chan, 2019: Climate change and tropical cyclone trend. *Nature*, **570**, E3–E5, https://doi.org/10.1038/s41586-019-1222-3.

Peduzzi, P., B. Chatenoux, H. Dao, A. D. Bono, C. Herold, J. Kossin, F. Mouton, and O. Nordbeck, 2012: Global trends in tropical cyclone risk. *Nat. Climate Change*, **2**, 289–294, https://doi.org/10.1038/nclimate1410.

Shan, K., and X. Yu, 2020: A simple trajectory model for climatological study of tropical cyclones. *J. Climate*, **33**, 7777–7786, https://doi.org/10.1175/JCLI-D-20-0285.1.

——, and ——, 2021: Variability of tropical cyclone landfalls in China. *J. Climate*, **34**, 9235–9247, https://doi.org/10.1175/JCLI-D-21-0031.1.

Shi, Y., Y. Du, Z. Chen, and W. Zhou, 2020: Occurrence and impacts of tropical cyclones over the southern South China Sea. *Int. J. Climatol.*, **40**, 4218–4227, https://doi.org/10.1002/joc.6454.

Song, J.-J., Y. Wang, and L. Wu, 2010: Trend discrepancies among three best track data sets of western North Pacific tropical cyclones. *J. Geophys. Res.*, **115**, D12128, https://doi.org/10.1029/2009JD013058.

Sun, Y., Z. Zhong, L. Yi, T. Li, M. Chen, H. Wan, Y. Wang, and K. Zhong, 2015: Dependence of the relationship between the tropical cyclone track and western Pacific subtropical high intensity on initial storm size: A numerical investigation. *J. Geophys. Res. Atmos.*, **120**, 11 451–11 467, https://doi.org/10.1002/2015JD023716.

Tu, J.-Y., C. Chou, and P.-S. Chu, 2009: The abrupt shift of typhoon activity in the vicinity of Taiwan and its association with western North Pacific–East Asian climate change. *J. Climate*, **22**, 3617–3628, https://doi.org/10.1175/2009JCLI2411.1.

Wang, C., 2019: Three-ocean interactions and climate variability: A review and perspective. *Climate Dyn.*, **53**, 5119–5136, https://doi.org/10.1007/s00382-019-04930-x.

——, and B. Wang, 2021: Impacts of the South Asian high on tropical cyclone genesis in the South China Sea. *Climate Dyn.*, **56**, 2279–2288, https://doi.org/10.1007/s00382-020-05586-8.

——, L. Wu, J. Lu, Q. Liu, H. Zhao, W. Tian, and J. Cao, 2020: Interannual variability of the basinwide translation speed of tropical cyclones in the western North Pacific. *J. Climate*, **33**, 8641–8650, https://doi.org/10.1175/JCLI-D-19-0995.1.

Wang, L., R. Huang, and R. Wu, 2013: Interdecadal variability in tropical cyclone frequency over the South China Sea and its association with the Indian Ocean sea surface temperature. *Geophys. Res. Lett.*, **40**, 768–771, https://doi.org/10.1002/grl.50171.

Wu, B., T. J. Zhou, and T. Li, 2009: Seasonally evolving dominant interannual variability modes of East Asian climate. *J. Climate*, **22**, 2992–3005, https://doi.org/10.1175/2008JCLI2710.1.

Wu, L., and B. Wang, 2004: Assessing impacts of global warming on tropical cyclone tracks. *J. Climate*, **17**, 1686–1698, https://doi.org/10.1175/1520-0442(2004)017<1686:AIOGWO>2.0.CO;2.

——, and H. Zhao, 2012: Dynamically derived tropical cyclone intensity changes over the western North Pacific. *J. Climate*, **25**, 89–98, https://doi.org/10.1175/2011JCLI4139.1.

——, and C. Wang, 2015: Has the western pacific subtropical high extended westward since the late 1970s? *J. Climate*, **28**, 5406–5413, https://doi.org/10.1175/JCLI-D-14-00618.1.

——, and X. Chen, 2016: Revisiting the steering principal of tropical cyclone motion in a numerical experiment. *Atmos. Chem. Phys.*, **16**, 14 925–14 936, https://doi.org/10.5194/acp-16-14925-2016.

——, B. Wang, and S. Geng, 2005: Growing typhoon influences on East Asia. *Geophys. Res. Lett.*, **32**, L18703, https://doi.org/10.1029/2005GL022937.

Xie, S.-P., K. Hu, J. Hafner, H. Tokinaga, Y. Du, G. Huang, and T. Sampe, 2009: Indian Ocean capacitor effect on Indo–western Pacific climate during the summer following El Niño. *J. Climate*, **22**, 730–747, https://doi.org/10.1175/2008JCLI2544.1.

Yamaguchi, M., J. C. L. Chan, I.-J. Moon, K. Yoshida, and R. Mizuta, 2020: Global warming changes tropical cyclone translation speed. *Nat. Commun.*, **11**, 47, https://doi.org/10.1038/s41467-019-13902-y.

Ying, M., W. Zhang, H. Yu, X. Lu, J. Feng, Y. Fan, Y. Zhu, and D. Chen, 2014: An overview of the China Meteorological Administration tropical cyclone database. *J. Atmos. Oceanic Technol.*, **31**, 287–301, https://doi.org/10.1175/JTECH-D-12-00119.1.

Zhang, Q., L. Wu, and Q. Liu, 2009: Tropical cyclone damages in China 1983–2006. *Bull. Amer. Meteor. Soc.*, **90**, 489–496, https://doi.org/10.1175/2008BAMS2631.1.

Zhao, H. K., L. G. Wu, and W. C. Zhou, 2009: Observational relationship of climatologic beta drift with large-scale environmental flows. *Geophys. Res. Lett.*, **36**, L18809, https://doi.org/10.1029/2009GL040126.

Zhao, J., R. Zhan, and Y. Wang, 2018: Global warming hiatus contributed to the increased occurrence of intense tropical cyclones in the coastal regions along East Asia. *Sci. Rep.*, **8**, 6023, https://doi.org/10.1038/s41598-018-24402-2.

Zheng, M., and C. Wang, 2022: Interdecadal changes of tropical cyclone intensity in the South China Sea. *Climate Dyn.*, **60**, 409–425, https://doi.org/10.1007/s00382-022-06305-1.

Zhou, T., and Coauthors, 2009: Why the western Pacific subtropical high has extended westward since the late 1970s. *J. Climate*, **22**, 2199–2215, https://doi.org/10.1175/2008JCLI2527.1.